BIOCHEMISTRY
including biophysical chemistry & molecular biology
Rapid Report

Biochemistry **2011,** *50,* 1429–1431 1429
DOI: 10.1021/bi102057m

Large Favorable Enthalpy Changes Drive Specific RNA Recognition by RNA Recognition Motif Proteins†

Krystle J. McLaughlin, Jermaine L. Jenkins, and Clara L. Kielkopf*

Department of Biochemistry and Biophysics, University of Rochester School of Medicine and Dentistry, Rochester, New York 14642, United States

Received December 24, 2010; Revised Manuscript Received January 20, 2011

ABSTRACT: The RNA recognition motif (RRM) is a prevalent class of RNA binding domains. Although a number of RRM/RNA structures have been determined, thermodynamic analyses are relatively uncommon. Here, we use isothermal titration calorimetry to characterize single-stranded (ss)RNA binding by four representative RRM-containing proteins: (i) U2AF^{65}, (ii) SXL, (iii) TIA-1, and (iv) PAB. In all cases, ssRNA binding is accompanied by remarkably large favorable enthalpy changes (−30 to −60 kcal mol^{-1}) and unfavorable entropy changes. Alterations of key RRM residues and binding sites indicate that under the nearly physiological conditions of these studies, large thermodynamic changes represent a signature of specific ssRNA recognition by RRMs.

The RNA recognition motif (RRM) is an abundant domain among proteins with central roles in post-transcriptional gene regulation (*1*) (Figure 1). Multiple RRMs often occur per polypeptide. For example, tandem RRMs of splicing factors U2AF^{65}, TIA-1, and SXL recognize U-rich pre-mRNA sites (*2*, *3*). The poly(A) binding protein (PAB) enhances translation following RRM-mediated recognition of the mRNA tail (*4*). Beyond the well-established role of canonical RRMs in binding RNA, RRM variants such as the U2AF homology motif (UHM) are dedicated to protein/protein interactions (*5*). This breadth of functions illustrates the importance of elucidating the structural and thermodynamic forces responsible for RRM interactions.

Despite extensive structural and functional investigations of RRMs, full thermodynamic characterizations of the enthalpy and entropy changes during RRM/RNA binding are scarce. A thorough characterization of RNA binding by an RRM has been completed for the U1A splicing factor (*6*). However, this rare example focuses on a single RRM binding a single-stranded (ss)RNA site within a stem loop, which differs from the prevalent systems of multiple RRMs recognizing unstructured ssRNAs. Enthalpy and entropy changes of ssRNA binding have been determined for a number of unrelated domains, including Hfq, GLD-1, *trp* attenuation protein (TRAP), tristetraprolin, and T4 translational regulatory protein (*7*−*11*). Given the diversity of these domain classes, it is unsurprising that no common thermodynamic themes of ssRNA binding have emerged to date. In contrast, protein/protein, protein/ligand, and protein/DNA interactions have been investigated in depth.

Previously, we found a large favorable enthalpy change (ΔH) and a large unfavorable entropy change ($-T\Delta S$) for the recognition of poly(U) by the tandem RRMs of U2AF^{65} (ΔH = −70 kcal mol^{-1}; $-T\Delta S$ = 61 kcal mol^{-1}) (*12*). Notably, these enthalpy and entropy changes were similar in magnitude to those observed for the single other example of RRM/RNA binding [U1A RRM/RNA stem loop (ΔH = −68 kcal mol^{-1}; $-T\Delta S$ = 58 kcal mol^{-1})] (*6*). To explore the generality of these observations for other RRM-containing proteins, we used isothermal titration calorimetry (ITC) to determine the enthalpy and entropy changes of ssRNA binding by four RRM-containing proteins: U2AF^{65}, SXL, TIA-1, and PAB. Constructs composed of two consecutive RRMs represented the major sites of RNA recognition for each protein (U2AF^{65} RRM12U, SXL RRM12, TIA-1 RRM23, and PAB RRM12) (*2*, *3*, *14*) (Figure 1C). To allow future comparison with higher-order complexes, the U2AF^{65} construct includes a C-terminal UHM that lacks detectable RNA affinity (*5*).

The ability of U2AF^{65}, SXL, and TIA-1 to recognize comparable U-rich sequences offered the opportunity for comparison of various RRM-containing proteins binding identical RNA sites (*3*, *15*). We preferred a poly(U) binding site for ITC, because this sequence is expected to lack (i) intra- or intermolecular secondary structures or (ii) multiple nonidentical binding sites that would complicate analyses. The optimal, poly(U) site of U2AF^{65} is well-established (*2*, *16*). We verified the poly(U) preferences of SXL and TIA-1 by fluorescence anisotropy (Figure S1 of the Supporting Information). Both splicing factors bound a 20-uridine (U_{20}) RNA with higher affinity than their natural splice sites (for SXL RRM12, K_D equals 7 ± 3 nM for U_{20} vs 47 ± 10 nM for the *tra* splice site; for TIA-1 RRM23, K_D equals 33 ± 6 nM for U_{20} vs 118 ± 16 nM for the *fas* splice site). Likewise, a 20-adenosine RNA (A_{20}) is similar in length to the repeating units of PAB/poly(A) mRNA tail complexes (*17*) and represents a specific PAB binding site for direct comparison with U_{20} RNAs. We subsequently focused on the U_{20} and A_{20} RNA binding sites.

Because the HEPES buffer used previously was replaced with BES here (to take advantage of a lower heat capacity change of ionization), we repeated the U2AF^{65} RRM12U/U_{20} titrations in BES for comparison (Figure S2A of the Supporting Information). Consistent with a mere 1 kcal mol^{-1} difference in the enthalpies of buffer ionization (*18*), the results agreed within error (ΔH = −61.3 ± 10.8 kcal mol^{-1}; $-T\Delta S$ = 53.0 ± 10.7 kcal mol^{-1}) (Table S1 of the Supporting Information). Large enthalpy and entropy changes were also found for specific RNA recognition by SXL, TIA-1, and PAB (for SXL RRM12/U_{20}, ΔH = −35.3 ± 2.9 kcal mol^{-1} and $-T\Delta S$ = 25.6 ± 2.8 kcal mol^{-1}; for TIA-1 RRM23/U_{20}, ΔH = −29.6 ± 0.5 kcal mol^{-1} and $-T\Delta S$ = 20.0 ± 0.5 kcal mol^{-1}; for PAB RRM12/A_{20}, ΔH = −29.3 ± 1.5

†This work was supported by the National Institutes of Health (Grant GM070503 to C.L.K.).
*To whom correspondence should be addressed. E-mail: clara_kielkopf@urmc.rochester.edu. Phone: (585) 273-4799. Fax: (585) 275-6007.

Published on Web 01/24/2011

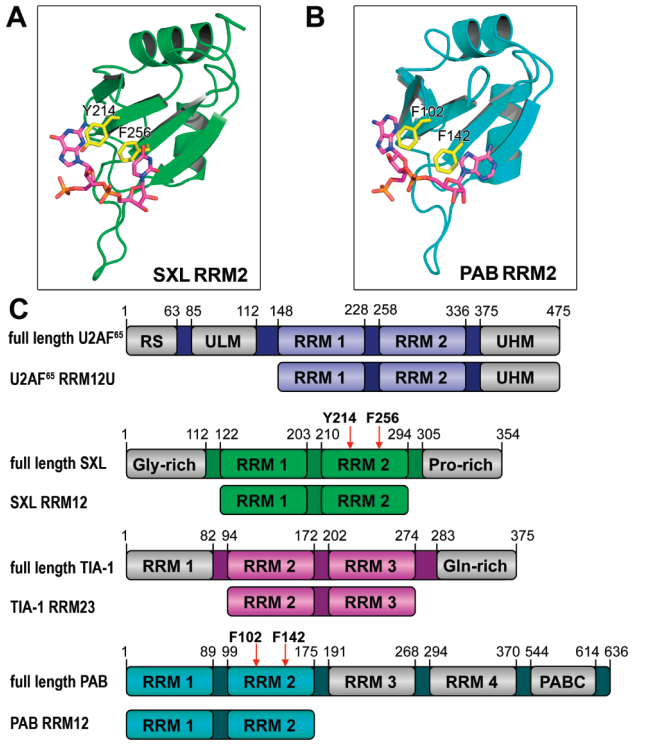

FIGURE 1: Structures of the second RRMs of (A) SXL (Protein Data Bank entry 1B7F) or (B) PAB (Protein Data Bank entry 1CVJ). RNP residues altered by mutagenesis are colored yellow. (C) U2AF^{65}, TIA-1, SXL, and PAB domain organization and constructs used in this study. RRM, RNA recognition motif; RS, arginine-serine-rich domain; ULM, UHM ligand motif; UHM, U2AF homology motif; Gly-rich, glycine-rich domain; Pro-rich, proline-rich domain; Gln-rich, glutamine-rich domain; PABC, peptide-binding domain.

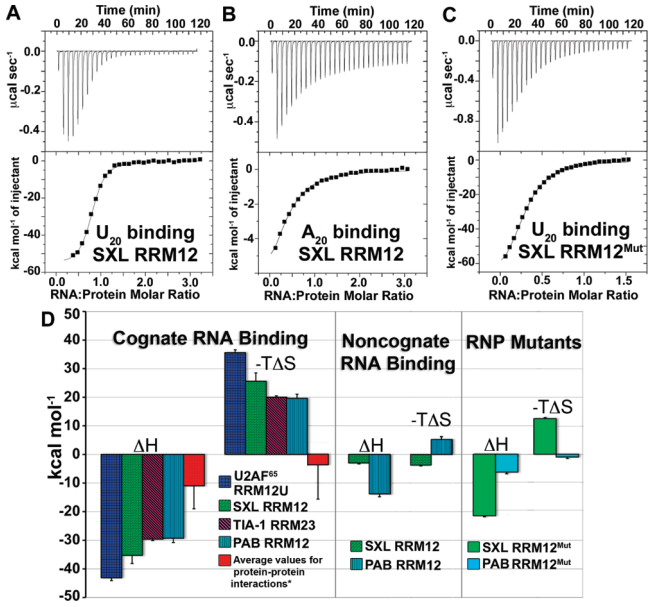

FIGURE 2: Representative isotherms for titration of (A) U_{20} RNA into SXL RRM12, (B) A_{20} RNA into SXL RRM12, and (C) U_{20} RNA into SXL RRM12^{Mut} in 100 mM NaCl and 25 mM BES (pH 7.4) at 303 K. All other isotherms are represented in the Supporting Information. (D) Bar graph representations of thermodynamic changes. The left panel shows specific RNA binding by wild-type RRM-containing proteins: U2AF^{65} RRM12U/U_{20}, SXL RRM12/U_{20}, TIA-1 RRM23/U_{20}, and PAB RRM12/A_{20}. Asterisks denote averaged nonredundant enthalpy (http://www.bioinfodatabase.com/pint/) and entropy (*13*) changes for protein/protein interactions. The middle panel shows noncognate RNA binding: SXL RRM12/A_{20} and PAB RRM12/U_{20}. The right panel shows RNP mutant proteins: SXL RRM12^{Mut}/U_{20} and PAB RRM12^{Mut}/A_{20}.

kcal mol^{-1} and $-T\Delta S$ = 19.6 ± 1.5 kcal mol^{-1}) (Figure 2 and Figure S2 and Table S1 of the Supporting Information). These results indicated that, considering the U1A RRM, five unrelated RRM-containing proteins that are <25% identical in sequence exhibited large favorable enthalpy changes and unfavorable entropy changes for recognition of diverse RNA sites (Figure 2).

Control titrations of U_{20} or A_{20} RNAs into buffer demonstrated that the heats of RNA dilution were not responsible for the apparent enthalpy and entropy changes (Figure S3A,B of the Supporting Information). To further ensure that the observed values did not depend on the configuration of the experiment, "reverse" titrations of SXL in the syringe into U_{20} RNA in the sample cell yielded similar enthalpy and entropy changes (ΔH = −43.6 ± 1.5 kcal mol^{-1}; $-T\Delta S$ = 33.9 ± 1.6 kcal mol^{-1}) as the "forward" titrations of U_{20} RNA into SXL (Figure S3C and Table S1 of the Supporting Information).

To the best of our knowledge, comparably large enthalpy and entropy changes for ssRNA recognition have been documented for only two cases besides RRMs: the Sm-like fold of Hfq [ΔH = −41 kcal mol^{-1} and $-T\Delta S$ = 30 kcal mol^{-1} for poly(A)] (*7*) and a CCCH-zinc finger of tristetraprolin (ΔH = −46 kcal mol^{-1} and $-T\Delta S$ = 35 kcal mol^{-1} for an AU-rich element) (*10*). Large, exothermic enthalpy changes also are observed for the well-studied case of ssDNA binding by SSB [ΔH = −70 kcal mol^{-1} for poly(T)] (*19*). In contrast, other characterized motifs bind ssRNA with moderate enthalpy and entropy changes (*8*, *11*) and can be entropically driven (*9*).

We next investigated the possible influence of proton exchange with the surrounding medium during formation of the RRM/RNA complex. To avoid possible competition between phosphate buffer and binding sites for the phosphodiester RNA backbone, we took advantage of the different ionization enthalpies of Tris compared with BES buffers (ΔH_i for Tris equals 11.7 kcal mol^{-1}; ΔH_i for BES equals 6.0 kcal mol^{-1}; $\Delta\Delta H$ = 5.7 kcal mol^{-1} per proton transfer) (*18*, *20*). Enthalpy changes for the representative SXL RRM12/U_{20} system were the same within error when measured in Tris compared with BES buffers (ΔH^{Tris} = −39.4 ± 0.2 kcal mol^{-1}) (Figure S4 and Table S1 of the Supporting Information). This result demonstrated that proton exchange was not responsible for the large observed magnitudes of the enthalpy and entropy changes.

We then examined whether the enthalpy and entropy changes depended on formation of specific RRM/RNA contacts (Figure 2 and Figure S5 of the Supporting Information). We focused on SXL and PAB for these experiments, because the affinities of these proteins for nonspecific RNAs were sufficiently high to remain within the reliable range for ITC measurements, and structures of the RNA complexes were known. For SXL RRM12, the magnitude of the enthalpy changes became nearly 90% less favorable for nonspecific A_{20} binding (ΔH = −3.1 ± 0.3 kcal mol^{-1}). Indeed, the SXL RRM12/A_{20} binding reaction became entropically favorable ($-T\Delta S$ = −3.7 ± 0.3 kcal mol^{-1}). The magnitudes of the enthalpy and entropy changes also decreased for nonspecific RNA binding by PAB RRM12 (ΔH = −13.8 ± 0.8 kcal mol^{-1}; $-T\Delta S$ = 5.3 ± 0.5 kcal mol^{-1}). Hence, the large enthalpy and entropy changes appeared to depend on specific RNA contacts by the RRM fold. Because nonspecific RNA binding often depends on favorable electrostatic interactions, this result further suggested that the release of counterions by complex formation was

unlikely to dominate the observed enthalpy and entropy changes. Accordingly, relatively few RRM/RNA salt bridges are evident among the proteins studied here (*21*−*23*) [approximately four compared with 23 for a representative salt-dependent complex, IHF/dsDNA (*24*)].

To further investigate the role of specific RNA contacts, we mutated conserved aromatic residues in the characteristic ribonucleoprotein motifs (RNP1 and RNP2) (Figure 1). These residues stack with RNA bases in the majority of canonical RRM structures, including SXL and PAB (*22*, *23*). Double mutations, F256A and Y214A in SXL RRM2 (SXL $RRM12^{Mut}$) and F102A and F142A in PAB RRM2 (PAB $RRM12^{Mut}$), decreased the enthalpy and entropy changes of target RNA binding relative to the wild-type counterparts and converted the PAB $RRM12^{Mut}/A_{20}$ interaction into an entropically favorable interaction (for SXL $RRM12^{Mut}/U_{20}$, $\Delta H = -22.3 \pm 0.4$ kcal mol^{-1} and $-T\Delta S = 14.5 \pm 0.4$ kcal mol^{-1}; for PAB $RRM12^{Mut}/A_{20}$, $\Delta H = -6.4 \pm 0.6$ kcal mol^{-1} and $-T\Delta S = -1.0 \pm 0.5$ kcal mol^{-1}) (Figure 2 and Figure S6 and Table S1 of the Supporting Information).

On the basis of our results for the SXL and PAB mutants, base stacking by conserved RNP residues contributes to the large thermodynamic changes for RRM/RNA interactions. In support of this conclusion, π stacking interactions are often enthalpically favorable (*25*, *26*). Notably, Hfq and tristetraprolin, which exhibit large enthalpy and entropy changes for ssRNA binding, like the RRM-containing proteins engage in extensive π stacking between aromatic side chains and the RNA bases (*27*, *28*). Similarly, aromatic SSB side chains stack with bound ssDNA bases (*29*), and site-directed mutagenesis of these residues reduces the enthalpy and entropy changes for nucleic acid binding (*30*). In contrast, GLD-1 and TRAP, which lack large favorable enthalpy and unfavorable entropy changes for ssRNA binding, also lack extensive contacts between aromatic side chains and nucleic acid bases (*31*, *32*). Thus, the conservation of the RNP motifs provides a rationale for the shared thermodynamic signature of large favorable enthalpy changes among RRM/RNA complexes characterized to date. Future studies will tell whether this theme continues to hold for the many diverse members of the RRM family and for other nucleic acid-binding domains.

ACKNOWLEDGMENT

We thank D. Turner, B. Miller, and V. Frasca for insightful discussions.

SUPPORTING INFORMATION AVAILABLE

Table S1, Figures S1−S5, and supplementary methods. This material is available free of charge via the Internet at http://pubs.acs.org.

REFERENCES

1. Maris, C., Dominguez, C., and Allain, F. H. (2005) *FEBS J. 272*, 2118–2131.
2. Singh, R., Banerjee, H., and Green, M. R. (2000) *RNA 6*, 901–911.
3. Dember, L. M., Kim, N. D., Liu, K. Q., and Anderson, P. (1996) *J. Biol. Chem. 271*, 2783–2788.
4. Mangus, D. A., Evans, M. C., and Jacobson, A. (2003) *Genome Biol. 4*, 223.
5. Kielkopf, C. L., Lücke, S., and Green, M. R. (2004) *Genes Dev. 18*, 1513–1526.
6. Williams, D. J., and Hall, K. B. (1996) *J. Mol. Biol. 257*, 265–275.
7. Mikulecky, P. J., Kaw, M. K., Brescia, C. C., Takach, J. C., Sledjeski, D. D., and Feig, A. L. (2004) *Nat. Struct. Mol. Biol. 11*, 1206–1214.
8. Ryder, S. P., Frater, L. A., Abramovitz, D. L., Goodwin, E. B., and Williamson, J. R. (2004) *Nat. Struct. Mol. Biol. 11*, 20–28.
9. Baumann, C., Otridge, J., and Gollnick, P. (1996) *J. Biol. Chem. 271*, 12269–12274.
10. Brewer, B. Y., Malicka, J., Blackshear, P. J., and Wilson, G. M. (2004) *J. Biol. Chem. 279*, 27870–27877.
11. Webster, K. R., and Spicer, E. K. (1990) *J. Biol. Chem. 265*, 19007–19014.
12. Jenkins, J. L., Shen, H., Green, M. R., and Kielkopf, C. L. (2008) *J. Biol. Chem. 283*, 33641–33649.
13. Stites, W. E. (1997) *Chem. Rev. 97*, 1233–1250.
14. Burd, C. G., Matunis, E. L., and Dreyfuss, G. (1991) *Mol. Cell. Biol. 11*, 3419–3424.
15. Singh, R., Valcarcel, J., and Green, M. R. (1995) *Science 268*, 1173–1176.
16. Coolidge, C. J., Seely, R. J., and Patton, J. G. (1997) *Nucleic Acids Res. 25*, 888–896.
17. Baer, B. W., and Kornberg, R. D. (1980) *Proc. Natl. Acad. Sci. U.S.A. 77*, 1890–1892.
18. Fukada, H., and Takahashi, K. (1998) *Proteins 33*, 159–166.
19. Ferrari, M. E., and Lohman, T. M. (1994) *Biochemistry 33*, 12896–12910.
20. Bernhard, S. A. (1956) *J. Biol. Chem. 218*, 961–969.
21. Sickmier, E. A., Frato, K. E., Shen, H., Paranawithana, S. R., Green, M. R., and Kielkopf, C. L. (2006) *Mol. Cell 23*, 49–59.
22. Handa, N., Nureki, O., Kurimoto, K., Kim, I., Sakamoto, H., Shimura, Y., Muto, Y., and Yokoyama, S. (1999) *Nature 398*, 579–585.
23. Deo, R. C., Bonanno, J. B., Sonenberg, N., and Burley, S. K. (1999) *Cell 98*, 835–845.
24. Holbrook, J. A., Tsodikov, O. V., Saecker, R. M., and Record, M. T., Jr. (2001) *J. Mol. Biol. 310*, 379–401.
25. Mascotti, D. P., and Lohman, T. M. (1992) *Biochemistry 31*, 8932–8946.
26. Makhatadze, G. I., and Privalov, P. L. (1994) *Biophys. Chem. 50*, 285–291.
27. Schumacher, M. A., Pearson, R. F., Moller, T., Valentin-Hansen, P., and Brennan, R. G. (2002) *EMBO J. 21*, 3546–3556.
28. Hudson, B. P., Martinez-Yamout, M. A., Dyson, H. J., and Wright, P. E. (2004) *Nat. Struct. Mol. Biol. 11*, 257–264.
29. Raghunathan, S., Kozlov, A. G., Lohman, T. M., and Waksman, G. (2000) *Nat. Struct. Biol. 7*, 648–652.
30. Kerr, I. D., Wadsworth, R. I., Cubeddu, L., Blankenfeldt, W., Naismith, J. H., and White, M. F. (2003) *EMBO J. 22*, 2561–2570.
31. Valverde, R., Edwards, L., and Regan, L. (2008) *FEBS J. 275*, 2712–2726.
32. Antson, A. A., Dodson, E. J., Dodson, G., Greaves, R. B., Chen, X., and Gollnick, P. (1999) *Nature 401*, 235–242.